tions of transcriptional activity of the host sequences flanking the provirus support the possibility that expression of the *neo* gene in Glob 1 mice may be due to the chromosomal position of the provirus. Globin expression in the nonhematopoietic tissues may in turn be due to activation of the internal promoter by the viral LTR.

The analysis of the three strains of transgenic mice presented in this report provides the first demonstration that retroviruses can be used for the introduction and tissue-specific expression of foreign genes into the mouse germ line. Our results indicate that a gene under the control of an internal promoter and transduced by a retroviral vector is responsive to *trans*-acting developmental signals, resulting in tissue-specific gene activation. Similar vector constructs expressing the gene of interest from an internal promoter may not only be appropriately expressed after transfer into mouse embryos, but may also function properly after introduction into stem cells of other lineages such as the hematopoietic system.

REFERENCES AND NOTES

1. R. D. Palmiter and R. L. Brinster, *Cell* **41**, 343 (1985).
2. R. E. Hammer, R. D. Palmiter, R. L. Brinster, *Nature (London)* **311**, 65 (1984); M. Le Meur, P. Gerlinger, C. Benoist, D. Mathis, *ibid.* **316**, 38 (1985); K. Yamamura *et al.*, *ibid.*, p. 67; F. Costantini, K. Chada, J. Magram, *Science* **233**, 1192 (1986).
3. R. Jaenisch, *Proc. Natl. Acad. Sci. U.S.A.* **73**, 1260 (1976); R. Jaenisch *et al.*, *Cell* **24**, 519 (1981); P. Soriano and R. Jaenisch, *ibid.* **46**, 19 (1986).
4. J. E. Dick, M. C. Magli, D. Huszar, R. A. Phillips, A. Bernstein, *Cell* **42**, 71 (1985); G. Keller, C. Paige, E. Gilboa, E. F. Wagner, *Nature (London)* **318**, 149 (1985); I. R. Lemischka, D. H. Raulet, R. C. Mulligan, *Cell* **45**, 917 (1986).
5. A. Schnieke, K. Harbers, R. Jaenisch, *Nature (London)* **304**, 315 (1983); K. Harbers, P. Soriano, U. Müller, R. Jaenisch, *ibid.*, in press.
6. R. Jaenisch, H. Fan, B. Crocker, *Proc. Natl. Acad. Sci. U.S.A.* **72**, 4008 (1975); C. Stewart, H. Stuhlmann, D. Jähner, R. Jaenisch, *ibid.* **79**, 4098 (1982); J. Gautsch and M. Wilson, *Cold Spring Harbor Conf. Cell Prolif.* **10**, 363 (1983); E. Barklis, R. C. Mulligan, R. Jaenisch, *Cell*, in press.
7. R. Jaenisch and D. Jähner, *Biochim. Biophys. Acta* **782**, 1 (1984); R. Jaenisch, D. Jähner, A. Schnieke, K. Harbers, *Proc. Natl. Acad. Sci. U.S.A.* **82**, 1451 (1985); D. Jähner, K. Haase, R. C. Mulligan, R. Jaenisch, *ibid.*, p. 6927.
8. D. Jähner *et al.*, *Nature (London)* **298**, 623 (1982); D. Jähner and R. Jaenisch, *Mol. Cell. Biol.* **5**, 2212 (1985).
9. D. Huszar *et al.*, *Proc. Natl. Acad. Sci. U.S.A.* **82**, 8587 (1985); H. Van der Putten *et al.*, *ibid.*, p. 6148; E. F. Wagner, G. Keller, E. Gilboa, U. Rüther, C. Stewart, *Cold Spring Harbor Symp. Quant. Biol.* **50**, 691 (1985); J. L. R. Rubenstein, J. F. Nicolas, F. Jacob, *Proc. Natl. Acad. Sci. U.S.A.* **83**, 366 (1986).
10. R. D. Cone, A. Weber-Benarous, D. Baorta, R. C. Mulligan, *Mol. Cell. Biol.*, in press.
11. S. F. Yu *et al.*, *Proc. Natl. Acad. Sci. U.S.A.* **83**, 3194 (1986).
12. D. A. Melton *et al.*, *Nucleic Acids Res.* **12**, 7035 (1984); P. Charnay *et al.*, *Cell* **38**, 251 (1984).
13. E. Lacy, S. Roberts, E. P. Evans, M. D. Burtenshaw, F. D. Costantini, *Cell* **34**, 343 (1983).
14. K. Chada *et al.*, *Nature (London)* **314**, 377 (1985); T. M. Townes, J. B. Lingrel, H. Y. Chen, R. L. Brinster, R. D. Palmiter, *EMBO J.* **4**, 1715 (1985); R. Krumlauf, R. E. Hammer, S. M. Tilghman, R. L. Brinster, *Mol. Cell. Biol.* **5**, 1639 (1985).
15. O. Choi and J. Engel, *Nature (London)* **323**, 731 (1986).
16. R. D. Palmiter, H. Y. Chen, R. L. Brinster, *Cell* **29**, 701 (1982).
17. C. L. Stewart, M. Vanek, E. F. Wagner, *EMBO J.* **4**, 3701 (1985).
18. T. M. Townes, H. Y. Chen, J. B. Lingrel, R. D. Palmiter, R. L. Brinster, *Mol. Cell. Biol.* **5**, 1977 (1985).
19. C. Cepko, B. Roberts, R. C. Mulligan, *Cell* **37**, 1053 (1984).
20. T. M. Shinnick, R. A. Lerner, J. G. Sutcliffe, *Nature (London)* **293**, 543 (1981).

21. We thank D. Grotkopp and R. Curry for excellent technical assistance, and our colleagues for critical comments on the manuscript. Supported by grant HD-19105 from the National Institutes of Health and by grant PO1-CA38497 from the National Cancer Institute.

14 August 1986; accepted 24 October 1986

Physical Theory of the Orientation of Astral Mitotic Spindles

MATTHEW BJERKNES

A physical theory was developed for mitotic spindle orientation. This is important because spindle position is known to determine the placement of the cleavage furrow separating the offspring of a mitosis. The theory is based on an equation for the force exerted on spindle poles by the interaction of astral microtubules with the cell surface. Expected spindle placements are positions of stable equilibrium where the net force and torque resulting from the action of the astral microtubules on the spindle poles is zero. The theory provides a novel physical explanation of cleavage patterns in the early embryo.

THE FIRST FEW MITOSES IN THE EARly embryo are often described as if they had crystalline perfection. "The plane of the first division is as a rule vertical; it passes through the main axis of the egg. The plane of the second division is also vertical and passes through the main axis, but it is at right angles to the first plane of cleavage. . . . The plane of the third division is at right angles to the first two planes and to the main axis of the egg. It is therefore horizontal or parallel to the equator of the egg" (*1*, p. 143). This is a textbook simplification; nonetheless it captures the essence of the pattern. Little is known about the physical basis of the orientation of mitosis in any cell (*2*). I describe a physical theory which, though simple, seems to capture the essence of the astral mitosis orientation process in general, including that which creates cleavage patterns.

The placement and orientation of the mitotic spindle determine the plane of cleavage in animal cells (*2, 3*). The problem of mitosis orientation may thus be profitably recast as the problem of spindle orientation. The spindle in anaphase may be viewed as a relatively rigid structure with an aster at each pole (Fig. 1). Asters are so named because the thousands (*4, 5*) of microtubules radiating from them give a starlike appearance (*2, 6, 7*). In anaphase the astral microtubules grow to reach the cell surface (*2, 5–7*). Hill and Kirschner (*8*) have proposed that the ability of a microtubule to exert a longitudinal force is due to polymerization of the tubule. This theory suggests that astral microtubules can exert a displacement force on the spindle pole, if they contact the cell surface or internal structures.

To calculate spindle position we must know the force exerted on the spindle poles by each astral microtubule. I assumed that the force per microtubule decreases with length squared. This relation was derived as follows. Hill and Kirschner (*8*) showed that the polymerization force has the form

$$-\frac{k_B T}{\ell_0} \ln \frac{C_e}{C_e^0} \sim 1 \times 10^{-6} \text{ dyne per tubule}$$

(k_B is Boltzmann's constant, T is temperature, ℓ_0 is the length of polymer per monomer, C_e is the concentration of free monomer at equilibrium, and C_e^0 is the critical concentration for polymerization). In their derivation, they assumed for simplicity that the tubules had no bending moment. This assumption is adequate for short tubules (<1 μm) or for situations where $C_e/C_e^0 \approx 1$. For long tubules, however, such as those found in the aster, buckling of the tubule would occur at forces weaker than the force available through polymerization (assuming no cross-linking of astral microtubules). The critical buckling force of a long thin rod of circular cross section is approximately $\pi^3 ER^4/(4L^2)$ where E is Young's modulus, R is the radius of the rod, and L is the length of the rod (*9*). Given that $E = 1.1 \times 10^8$ dyne cm^{-2} (*10*) and $R = 1.4 \times 10^{-6}$ cm, the critical buckling

Department of Anatomy, Medical Sciences Building, University of Toronto, Toronto, Ontario, Canada M5S 1A8.

force for a tubule 50 μm long would be about 10^{-10} dyne, about 1/10,000 of the maximum force the tubule could exert through polymerization. This force is sufficient, however, to displace the spindle.

The force necessary to rotate a sphere of radius r at radial velocity ω in an infinite fluid of viscosity η is $8\pi\eta r^3\omega$ (*11*). Thus, to a crude approximation, to rotate a spindle of 50-μm radius in cytoplasm of viscosity 0.1 g cm^{-1} sec^{-1} (*12*) at 1 radian $hour^{-1}$ requires a force of about 10^{-10} dyne. This is about the same as the force a 50-μm tubule can exert before buckling. It is plausible, therefore, that an aster with several thousand tubules attached could have a significant impact on spindle placement. Thus, as a simple approximation, an astral tubule ($\gg$1 μm) exerts at most its buckling force, which decreases with length squared (tubule buckling may also be important in discriminating between theories of other microtubule functions, for example, chromosome movement).

To calculate the net force on an aster we need to know not only the force per tubule, but also the density of tubules interacting with each point of the cell surface. Consider a patch of cell surface, dA, with unit normal $\hat{\mathbf{n}}$. The number of microtubules interacting with the patch will vary with distance from the aster and the angle between patch and tubules. In fact, since the microtubules radiate out from the aster, the density of tubules interacting with a patch will decrease with the square of the distance of the patch from the aster. If $\mathbf{r}$ is a vector representing a point on the cell surface, and $\mathbf{a}$ is a vector representing the aster, then $(\mathbf{r} - \mathbf{a})$ represents a vector running from the aster to the surface. If the q microtubules associated with the aster at $\mathbf{a}$ are uniformly distributed about the aster, then the density of tubules from that aster interacting with the surface element at $\mathbf{r}$ is

$$\frac{q(\mathbf{r} - \mathbf{a}) \cdot \hat{\mathbf{n}}}{4\pi \|(\mathbf{r} - \mathbf{a})\|^3}$$

Similarly, the component of force exerted, in the direction of the unit vector $\hat{\mathbf{i}}$, by a microtubule running from $\mathbf{a}$ to $\mathbf{r}$, is

$$-\frac{[\pi^3 ER^4(\mathbf{r} - \mathbf{a}) \cdot \hat{\mathbf{i}}]}{4\|(\mathbf{r} - \mathbf{a})\|^3}$$

Thus, the resultant force on a single aster within a cell is approximately

$$f_i = -\alpha \int\int_S \left[\frac{(\mathbf{r} - \mathbf{a}) \cdot \hat{\mathbf{i}}}{\|(\mathbf{r} - \mathbf{a})\|^3}\right] \left[\frac{(\mathbf{r} - \mathbf{a}) \cdot \hat{\mathbf{n}}}{\|(\mathbf{r} - \mathbf{a})\|^3}\right] dA$$

where $\alpha = q\pi^2 ER^4/16$. The first factor in the integral represents the force per tubule; the second factor is the number of tubules interacting with the surface element. Their product represents the force exerted on the aster by microtubules interacting with the surface element. The integral is over the surface of the cell, S, which may include internal structures (for example, a layer of yolk) in the surface that limits the aster. This means that cell shape is an important determinant of the force acting on an aster.

Equilibrium positions of an isolated aster in a cell are positions where the net force on the aster is zero. Simple intuition might lead to the conclusion that any force law for microtubules would yield essentially the same result as the law of inverse length squared assumed here. As long as a microtubule can "push," the same equilibrium point will be found. To demonstrate the fallacy of this argument, assume for the moment that the force generated per tubule is independent of tubule length. Then we would find that a fully developed aster placed in any position in a cell has zero net force acting on it, regardless of cell shape, because the force generated by the interaction of each tubule with the surface is canceled by the tubule on the opposite side of the aster. As a result, if microtubule force generation were independent of microtubule length, then no matter where the aster was put, it would stay (unless we consider more subtle statistical mechanical effects). Of course, if the aster was not fully developed at the outset of the experiment, then the aster would be displaced by the first tubules to contact the surface. The ultimate resting point of the aster would then be a complicated function of original aster position, microtubule force generation and growth rates, cytoplasmic viscosity, and cell shape. In contrast, under the law of inverse length squared, the law for force generation used here, a unique equilibrium position exists for an isolated aster within a simple closed surface regardless of initial conditions. This final equilibrium position depends only on cell shape.

It should be stressed that in all of the calculations performed I have assumed that the microtubules radiating from the aster are uniformly distributed and that microtubules can be treated in aggregate as though they formed a sort of a rubbery bag. In fact, microtubules are discrete objects, and there may well be some variability in the distribution of microtubules within the aster. Thus a more thorough treatment would start with the probability density function for microtubule placement within the aster and then proceed to a calculation of various moments (for example, mean and variance) of the final aster position. Nonetheless, since the density of astral microtubules is high and their distribution is fairly uniform (*2, 4–7*), the simplifying assumptions made here seem reasonable for a first approximation.

The astral equation yields forces of reasonable magnitude, as can be shown by calculating the dynamics of an aster interacting with a large planar surface. This provides an approximation to the early migration of the sperm aster and can be compared with known rates of sperm aster migration (*6*). A simple integration of the astral equation (*13*) shows that the net force on the aster should be perpendicular to the plane and of magnitude $\alpha\pi/(2h^2)$, where h is the distance of the aster from the plane. Stokes' law for the force on a sphere of radius p moving through a medium of viscosity η at velocity v is $6\pi\eta pv$ (*11*). Setting this equal to the force acting on the aster and solving for the velocity, we obtain

$$v(t) = dh(t)/dt = \frac{q(t)\pi^2 ER^4}{192\eta p[h(t)]^2}$$

$$= \frac{q\pi^2 ER^4}{\{1 + \exp[g(t' - t)]\}\{192\eta b[h(t)]^3\}}$$

where the last step follows from the assumptions (i) that the effective Stokes' radius, p, equals $bh(t)$ (b is a constant, which I take to be about 1), and (ii) that $q(t)$, the number of microtubules in the sperm aster at time t, is a logistic function,

$$q(t) = \frac{q}{1 + \exp[g(t' - t)]}$$

(t' is the time to development of one-half of the full complement of astral microtubules, and g is a constant that determines the rate of increase in tubule numbers). Solving the differential equation for $h(t)$ and substituting $h(t)$ back into the equation for sperm aster velocity, $v(t)$, yields

$$v(t) = \frac{M}{N\left\{4M\left[t + \frac{1}{g} \cdot \ln\frac{N}{1 + \exp(gt')}\right] + [h(0)]^4\right\}^{3/4}}$$

where $M = (q\pi^2 ER^4)/(192\eta b)$ and $N = 1 + \exp[g(t' - t)]$. The predicted rate of astral migration varies between 3×10^{-6} and 8×10^{-6} cm sec^{-1} (q = 2000; η = 0.1 g cm^{-1} sec^{-1}; t' = 480 seconds; g = 0.015 sec^{-1}; b = 1; and $h(0) = 4 \times 10^{-4}$ cm), which compares well with the 4.2×10^{-6} cm sec^{-1} measured in the sea urchin (*6*).

Before applying the theory to mitosis, it would be useful to calculate how the number of microtubules in a spherical cell, q, varies with cell radius, p. A simple relation exists if we can assume that cells have the same concentration, C, of free monomer regardless of cell size. If this is so, the total number of tubulin monomers in a cell is $m \cong 4\pi p^3 C/3 + kpq$, where k is the number

of monomers per unit length of microtubule. A cell of known radius p_1 would have $m_1 \cong 4\pi p_1^3 C/3 + kp_1q_1$. Solving for C,

$$C = \frac{3(m_1 - kp_1q_1)}{4\pi p_1^3} = \frac{3(m - kpq)}{4\pi p^3}$$

Solving for the number of tubules,

$$q = \frac{p^2q_1}{p_1^2} + \frac{m - p^3m_1/p_1^3}{kp}$$
$$\sim p^2q'$$

where $q' = q_1/p_1^2$ and $(m - p^3m_1/p_1^3)/(kp)$ is small. An estimate of $q' \cong 4$ (assuming p is in micrometers) can be obtained from the fact that for the sea urchin zygote, $p \cong 50$ μm and $q \cong 10^4$ (*4, 5*). Thus a cell of radius 5 μm should contain about 10^2 microtubules, whereas a cell of radius 16 μm should contain about 10^3 microtubules.

There is an aster at each end of the mitotic spindle; so both a displacement force and a torque act on the spindle. Expected spindle placements are positions of stable equilibrium where the net force and torque on the spindle are zero (*14*). If the asters in the cell are similar, the details of the constants that make up α are unimportant because we are only interested in the equilibrium positions of the spindle. Even if the asters are dissimilar, we still require only their relative, not their absolute, "strength." This is an important advantage of the theory, if the cell has symmetric asters; the theory needs no detail beyond cell geometry and spindle length. If correct, the theory should be applicable to astral mitosis in general, which includes the majority of animal and some plant cells. The anastral cells found in higher vascular plants have evolved other mechanisms to effect mitotic orientation; spindle position apparently plays no role. Instead the preprophase band seems to indicate the ultimate plane of cytokinesis (*15*), but it is not known what determines preprophase band placement.

Spindle positions in anastral mitoses (*2*) often do not correspond to what would be expected from the astral theory. In astral cells, the theory should work best in late anaphase. By late anaphase the spindle and astral fibers are fully developed (*5–7*) and cell geometry is relatively stable. I have assumed that the asters in a cell are identical and that cytoplasmic and surface properties affecting microtubule formation and stability are uniformly distributed. This need not be so in all cells (*7*). These effects may be incorporated into the theory if needed. For example, making the asters asymmetric by giving the two asters different values for α seems to explain many asymmetric mitoses (*2, 16*; Fig. 2, H and I).

I analyzed the amphibian cleavage pattern in detail as an interesting example of the application of the theory (the results are applicable to an analysis of the cleavage patterns in many nonamphibian species as well). The fertilized ovum was considered to be a sphere with a yolk layer of varying height (Fig. 1A). In each division, stable spindle positions and orientations were found by solving the astral equation for the appropriate cell geometry. The theory places the first spindle parallel to the yolk layer with the spindle centered on the axis of symmetry of the cell (Fig. 1A). This gives a vertical first cleavage (*17*). The second division occurs in hemispherical cells. In this case, the spindle is horizontal but parallel to the boundary between the cells (Fig. 1B). The cleavage plane induced by a spindle in this position would be vertical and perpendicular to the first cleavage plane, yielding four quarter spheres. Spindle orientation during the third cleavage depends on the

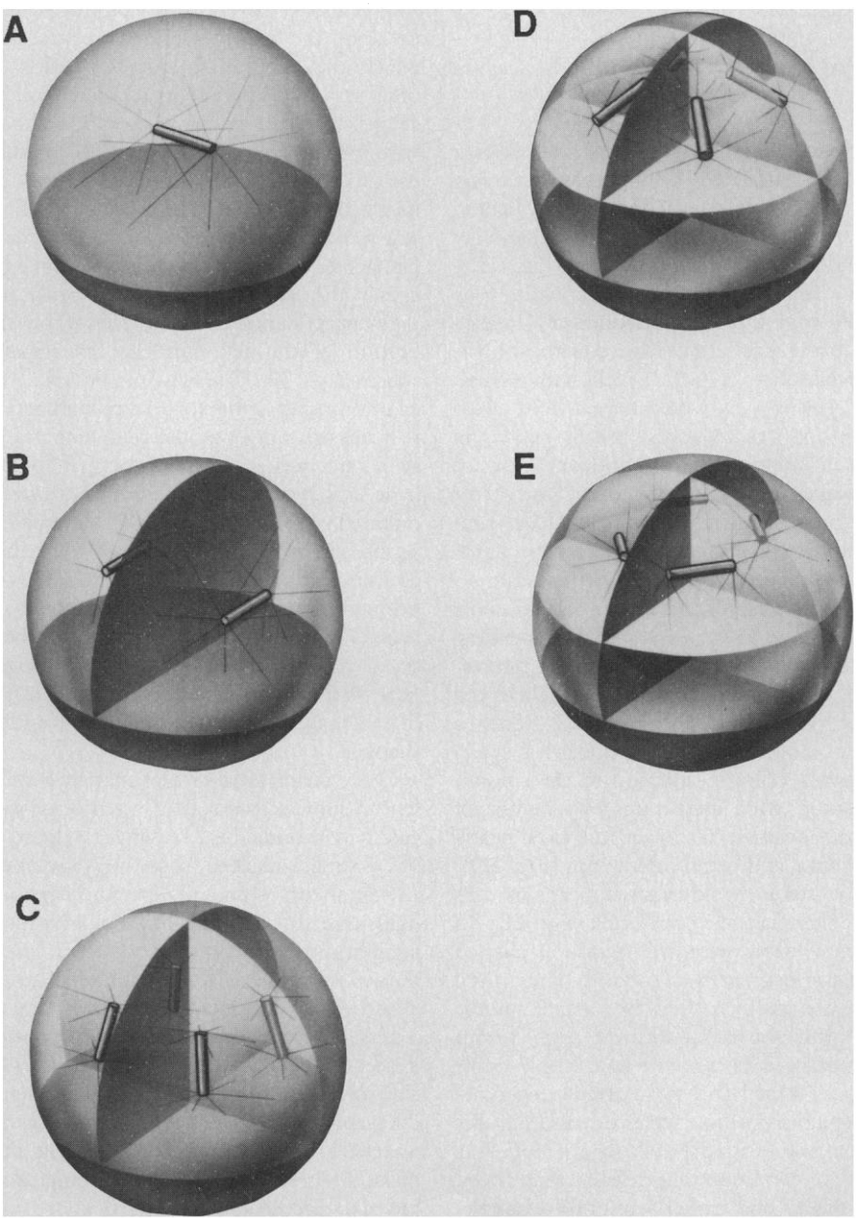

Fig. 1. Predicted spindle positions in a spherical embryo of diameter 1, spindle length 0.2, and an effective yolk layer filling the bottom third of the cell. The spindle positions shown are positions of stable equilibrium. The sequence approximates early development in *Xenopus laevis*. (A) Spindle is horizontal during first mitosis giving a vertical cleavage. (B) Spindles in second mitosis are horizontal but perpendicular to that in the first cleavage. This results in a vertical cleavage at right angles to the first cleavage plane. (C) Spindle in third mitosis is nearly vertical giving a horizontal third cleavage plane. (D and E) May be viewed as representing either the third mitosis in yolk-filled cells, or the fourth mitosis in animal pole cells (the new cell surface replaces the yolk layer in the latter instance). The spindle in a cell with this geometry has two stable positions, an approximately radial position (D) and a position aligned with the perimeter (E).

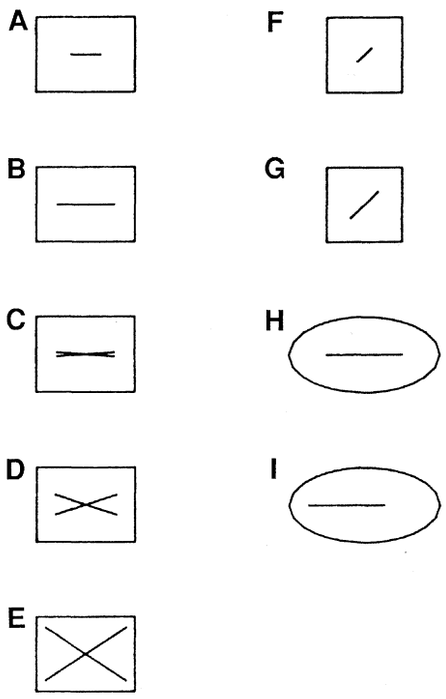

Fig. 2. (A to E) Idealized two-dimensional rectangular cells illustrating bifurcation of the equilibrium position of spindles with increasing spindle length but fixed cell geometry. In cells with spindles shorter than a critical length, only the horizontal position is stable (A and B). Beyond that length, the horizontal position becomes unstable and two new stable positions appear (C to E). With increasing spindle length the stable positions tend to be between opposite corners. This is the only stable orientation in a perfectly square cell (F and G). (H and I) Elliptical cell showing the effect of symmetric (H) versus asymmetric (I) asters. In (I) the aster on the left spindle pole is weaker than the aster on the right.

height of the yolk layer. If the yolk layer is low, the spindle will be almost vertical (Fig. 1C). As the yolk layer increases in height, the spindle moves higher in the cell and lies closer to the horizontal plane (Fig. 1D). Thus, cells with a low-placed yolk layer would have a nearly horizontal third cleavage plane just above the equator of the original sphere (Fig. 1C). Cells with increasing levels of yolk would have a third cleavage plane situated progressively higher in the cell and moving from horizontal toward vertical cleavage (with exceptions as noted). A comparison with the introductory paragraph demonstrates that the theory produces the prototypical cleavage pattern.

A useful test of the theory should come from the novel prediction that, depending on cell geometry and spindle length, bifurcations giving multiple stable equilibria can occur (Figs. 1, D and E, and 2). Such a situation occurs during the third cleavage in high-yolk cells. In addition to the smooth transition with increasing yolk height of spindle position from vertical to a nearly horizontal and radial orientation (Fig. 1D), a new stable equilibrium appears in cells more than half-filled with yolk (Fig. 1E). In the new stable state, the spindle is aligned with the perimeter of the cell. Thus a cell with this geometry has two stable spindle positions, one radial and one aligned with the surface. The existence of multiple stable states, and the fact that, for fixed cell geometry, spindle position varies dramatically depending on relative spindle length (Fig. 2, A to I) are two important differences between this theory and earlier work (for example, Hertwig's rule that the spindle lies in the direction of greatest protoplasmic mass; *2*).

A simple application of the theory to mitosis comes from experiments where spherical cells were given a cylindrical geometry (*3*). With a minimum of effort, it can be shown that relatively short spindles should lie along the axis of symmetry of the cell, which they appear to do. Repetition of other classical experiments that alter spherical geometry (*2*) or comparison of embryos with varying amounts of yolk (*18*) could be used to test the theory, if detailed measurements of cell geometry, yolk distribution, and spindle position were made. For example, gentle centrifugation of sea urchin eggs causes the diffusely distributed yolk and pigment granules to form a layer on the bottom of the cell, but the cell remains spherical (*2, 19*). The first spindle lies parallel to this layer. If the force of centrifugation is increased, however, the cell elongates. If the elongation is sufficient, the first spindle is no longer parallel to the layer but now is oriented vertically in the cell. This example is similar to the third cleavage described above. Unfortunately, the details of cell geometry after centrifugation are not available. A repetition of this sort of experiment could provide a good test of the theory, because the theory should predict the degree of cell elongation at which spindle position changes.

Other characteristics that may be important in some cells but that were not considered here include the following: (i) the stage of cytokinesis reached by previous divisions; (ii) the theory is an equilibrium theory and holds only if the spindle has time to achieve equilibrium before cytokinesis; and (iii) if the cell is yolk-filled and the spindle is small, a viscoelastic treatment of the yolk may be necessary. These effects can be incorporated if needed. Finally, while the theory may be able to predict spindle placement and hence the plane of cytokinesis, it does not necessarily reflect the final arrangement of cells after mitosis because extensive cell rearrangement can take place.

REFERENCES AND NOTES

1. I. Balinsky, *An Introduction to Embryology* (Saunders, Philadelphia, ed. 3, 1970).
2. T. H. Morgan, *Experimental Embryology* (Columbia Univ. Press, New York, 1927), pp. 487–490; E. B. Wilson, *The Cell in Development and Inheritance* (Macmillan, New York, 1928); B. C. Goodwin and L. E. H. Trainor, *J. Theor. Biol.* **86**, 757 (1980).
3. R. Rappaport and B. N. Rappaport, *J. Exp. Zool.* **234**, 167 (1985); R. Rappaport, *ibid.* **235**, 217 (1985); K. Kawamura, *Exp. Cell Res.* **106**, 127 (1977); I. Mabuchi, *Int. Rev. Cytol.* **101**, 175 (1986).
4. W. D. Cohen and L. I. Rebhun, *J. Cell Sci.* **6**, 159 (1970).
5. C. F. Asnes and T. E. Schroeder, *Exp. Cell Res.* **122**, 327 (1979).
6. See figures in T. L. Karr and B. M. Alberts, *J. Cell Biol.* **102**, 1494 (1986); T. H. Bestor and G. Schatten, *Dev. Biol.* **88**, 80 (1981).
7. D. G. Albertson, *Dev. Biol.* **101**, 61 (1984).
8. T. L. Hill and M. W. Kirschner, *Int. Rev. Cytol.* **78**, 1 (1982).
9. L. D. Landau and E. M. Lifshitz, *Theory of Elasticity* (Pergamon, New York, 1970), p. 98.
10. E was derived from Hill and Kirschner's constant a in their force law $F = a(L/N - L_0/N)$ (*8*, p. 45), which they estimate to be 1.1×10^4 dyne cm^{-1} (L and L_0 are microtubule length in the presence and absence of force, respectively, while N is the number of tubulin monomers in the tubule). This gives $(L = L_0)/L_0 = F/(a\ell_0) = 1.5 \times 10^{-3}$, when $F = 1 \times 10^{-6}$ dyne and $\ell_0 = 6.15 \times 10^{-8}$ cm ($\ell_0 = L_0/N$, the length of tubule per monomer). Converting this into the usual Young's modulus for a three-dimensional rod was done as follows, $F/(\pi R^2)$ dyne cm^{-2} $= 1.5 \times 10^{-3}$ E. Then, since $R = 1.4 \times 10^{-6}$ cm, $E \cong 1.1 \times 10^8$ dyne cm^{-2}.
11. S. H. Lamb, *Hydrodynamics* (Dover, New York, 1932), p. 589.
12. F. H. C. Crick and A. F. W. Hughes, *Exp. Cell Res.* **1**, 37 (1950); E. D. Salmon *et al.*, *J. Cell Biol.* **99**, 2157 (1984).
13. The force exerted on an aster by the interaction of the astral microtubules with an infinite plane is

$$-\alpha \int_0^{2\pi} \int_0^{\infty} \frac{-h^2\rho}{(\rho^2 + h^2)^3}\, d\rho d\theta = \frac{\alpha\pi}{2h^2}$$

where h is the height of the aster above the plane and ρ and θ are standard cylindrical coordinates. The error introduced by assuming an infinite surface of integration is small, as can be proved by comparing the result with that obtained from interaction with a circular disk of radius h, $3\alpha\pi/(8h^2)$. This is because the force exerted by tubules interacting with points on the plane far away from the aster is negligible.
14. A statistical mechanical approach could be used to calculate the probability of any given orientation for a fixed cell geometry. The problem is analogous to that of calculating the orientation of a dipole in an electric field; J. E. Meyer and M. G. Meyer, *Statistical Mechanics* (Wiley, New York, ed. 2, 1977), pp. 391–393.
15. S. C. Tiwari, S. M. Wick, R. E. Williamson, B. E. S. Gunning, *J. Cell Biol.* **99**, 63s (1984).
16. K. Dan, in *Cell Reproduction*, E. R. Dirksen, D. M. Prescott, C. F. Fox, Eds. (Academic Press, New York, 1978), pp. 557–561; M. Moreau, P. Guerrier, M. Dorée, *J. Exp. Zool.* **197**, 435 (1976); S. Schorderet-Slatkine, M. Schorderet, E. E. Baulieu, *Differentiation* **9**, 67 (1977).
17. The symmetry of the orientation of the first mitotic spindle about the cell axis could be broken in the correct direction by the perturbation of the yolk layer that is known to follow rotation of the cytoplasm after fertilization; A. W. Neff *et al.*, *J. Embryol. Exp. Morphol.* **80**, 197 (1984); J. Vincent, G. F. Oster, J. C. Gerhart, *Dev. Biol.* **113**, 484 (1986); R. P. Elinson, *Symp. Soc. Dev. Biol.* **38**, 217 (1980).
18. R. Rugh, *Experimental Embryology* (Burgess, Minneapolis, MN, 1965); E. M. Del Pino and B. Escobar, *J. Morphol.* **167**, 277 (1981).
19. E. B. Harvey, *The American* Arbacia *and Other Sea Urchins* (Princeton Univ. Press, Princeton, NJ, 1956), plate VIII.

20. I thank H. Cheng, R. Elinson, A. Forer, and J. Totafurno for helpful discussions. Supported by grants from the Medical Research Council of Canada and the Canadian Foundation for Ileitis and Colitis.

10 July 1986; accepted 10 October 1986